Short communication

Catalyst-free growth of large scale nitrogen-doped carbon spheres as efficient electrocatalysts for oxygen reduction in alkaline medium

Xuemei Zhou, Zhi Yang*, Huagui Nie, Zhen Yao, Lijie Zhang, Shaoming Huang**

Nanomaterials and Chemistry Key Laboratory, Wenzhou University, Wenzhou 325027, China

ARTICLE INFO

ABSTRACT

Nitrogen-doped carbon spheres (NCS) are synthesized by directly pyrolyzing a nebulized solution of xylene and ethylenediamine via a spray pyrolysis method, without using a catalyst. X-ray photoelectron spectroscopy (XPS) measurements confirm that the NCS only contain C, N and O. The electrocatalytic performances show that the NCS exhibit a high catalytic activity, long-term stability, and an excellent methanol tolerance for the oxygen reduction reaction (ORR) in an alkaline medium. This study successfully develops a new non-precious metal catalyst, which exhibits an excellent electrocatalytic performance, using a simple, cost-effective and scalable method. It also provides an increased fundamental understanding in the origins of ORR activity enhancements using N-doped carbon materials.

1. Introduction

The high cost and scarcity of the requisite noble metal materials have become a technological bottleneck for the industrial development of fuel cells (FCs) [1]. Reducing or replacing Pt-based catalysts is viewed as the long-term strategy for the development of FCs [2]. The development of novel non-precious metal catalysts (NPMC), which exhibit both high activity and practical durability, is one of the most active and competitive fields in chemistry and material science [3]. Dai et al. [4] reported that vertically aligned N-doped carbon nanotubes (CNTs) can act as an extremely efficient metal-free electrocatalysts for the oxygen reduction reaction (ORR). Various N-doped carbon materials (NCMs) [5–12], including single-walled carbon nanotubes, nanotube cups, ordered mesoporous graphitic arrays, and graphene have been developed as potential alternatives for Pt-based catalysts. Iron-based catalysts are usually used to prepare NCMs, such as in nanotube and graphene growth [4,6,8,10]. However, it is difficult to completely remove the catalyst particles from the NCM, even after tedious purification processes [13]. These metal particles could potentially affect the ORR performance. It is debated whether the C-N structure in NCMs plays a decisive role in the observed ORR activity enhancement. Although some metal-free NCM catalysts have been prepared

using nanocasting technology [9], SiO$_2$-catalytic chemical vapor deposition [5] and the hard template approach [11], these synthesis methods are not efficient and involve tiresome procedures. Furthermore, other residuals such as SiO$_2$ in these metal free catalysts can impact performance. In this regard, the development of NCMs with an excellent electrocatalytic performance, using a cost-effective catalyst-free synthesis method is of significant interest.

Herein, we report a simple catalyst-free synthesis method for the preparation of nitrogen-doped carbon spheres (NCS). We find that the NCS exhibit excellent catalytic activities, long-term stability, and a high methanol tolerance. The development of such catalyst-free NCS strongly supports the C-N structure having a decisive role in the ORR activity enhancement. Further clarification in terms of the ORR mechanism with NCMs is also important, along with elucidating the correlation between NCM structure and ORR performance. Because of the inherent advantages of the nebulized spray pyrolysis method, such as its simple scale-up [14], and the availability of raw material, this simple synthesis approach for NCS could have a significant economic impact on the next generation of cheap and sustainable FCs with alkaline electrolyte.

2. Experiment

2.1. Synthesis of nitrogen-doped carbon spheres via the spray pyrolysis method

NCS were directly synthesized via a spray pyrolysis method, which was depicted in our previous report [15]. In the experiment, xylene and ethylenediamine are the carbon and nitrogen sources,

* Corresponding author. Tel.: +86 577 8837 3064; fax: +86 577 8837 3017.
** Corresponding author.
  E-mail addresses: yang201079@126.com (Z. Yang), smhuang@wzu.edu.cn (S. Huang).

Table 1
Physical parameters, electrochemical properties and corresponding experimental data for various carbon spheres and a Pt/C catalyst.

Samples	Ratio of ethylenediamine and xylene (v/v)	Reaction time (min)	Diameter (nm)	Specific surface area ($m^2 g^{-1}$)	N content (wt.%)	Kinetic current density ($mA cm^{-2}$)	Number of electron transfer, n
CS	0	20	130–220	11.2	0	1.83	1.52
NCS-1	1:9	20	140–230	12.1	2.1	2.21	2.31
NCS-2	3:7	20	135–220	11.5	4.3	3.04	3.05
NCS-H	5:5	20	130–180	12.8	6.2	5.21	3.86
NCS-3	5:5	40	250–500	4.2	6.1	3.95	3.41
Pt/C						4.36	3.91

respectively. The solution is nebulized using a medical nebulizer and carried into a quartz tube at a temperature of 1000 °C. Argon is used as the carrier gas. Upon reaction completion, the solution flow is stopped and the furnace is cooled to room temperature with an argon flow. The samples are collected by peeling the deposited carbon materials from the quartz tube wall. The N content (from 0 to 6.2 wt.%) and sphere size (from 130 to 500 nm) for the NCS can be tuned by varying both the ratio of xylene and ethylenediamine as well as the reaction time. The resulting materials are denoted as CS (non-nitrogen carbon spheres), NCS-1, NCS-2, NCS-3 and NCS-H, respectively. Their physical parameters, electrochemical properties and corresponding experimental data are listed in Table 1.

2.2. Electrochemical characterization

Glassy carbon (GC) electrodes (3 mm diameter, CH Instrument Inc.) are polished with 0.3 and 0.05 μm alumina slurries, followed by rinsing with ultrapure water and ethanol. The electrodes are then sonicated in ultrapure water to remove any bound particles, rinsed thoroughly with ultrapure water and dried under a nitrogen stream. To prepare the working electrode, 1 mg of each sample is individually dispersed ultrasonically in 1 mL ethanol. Two microliters of the resulting suspension is dropped onto the GC surface at room temperature and the ethanol evaporated. Electrochemical measurements were performed using a computer-controlled potentiostat (CHI 760C, CH Instrument) with a typical three-electrode cell, equipped with gas flow systems. The NCS electrode is used as the working electrode, an Ag/AgCl (3 M KCl-filled) electrode as the reference electrode, and a platinum wire as the counter electrode. Moreover, to rule out the possibility that Pt metal (from Pt-counter electrode) might be responsible for the observed electrocatalytic activity of NCS-H, the electrochemical tests using Ni as counter electrode to replace Pt were also performed. It is found that these NCS show similar electrochemical performance whether the counter electrode is Ni or Pt. An aqueous solution of KOH (0.1 M) is used as the electrolyte for both normal cyclic and rotating disk electrode (RDE) voltammogram measurements. For comparison, a commercially available Pt/C catalyst (20 wt.% Pt supported on carbon black from Sigma, fuel cell grade) was used. A 1 mg mL^{-1} Pt/C suspension was also prepared, and 2 μL was taken and dropped onto the electrode surface.

2.3. Characterizations of physical parameters

X-ray diffraction (XRD) measurements were performed using Philips PW 1710 diffractometer with Cu Ka1 radiation. X-ray photoelectron spectroscopy (XPS) measurements were carried out with an ultra-high vacuum setup, equipped with a monochromatic Al Kα X-ray source and a high resolution Gammadata-Scienta SES 2002 analyzer. SEM images were obtained with a JSM-6700F field-emission scan electron microscope. Transmission electron microscopy (TEM) and high-resolution transmission electron microscopy (HRTEM) images were recorded with a JEOL-3010 instrument. Specific surface areas were measured using the Brunauer–Emmett–Teller (BET) method. The BET surface areas

of the samples were determined from N_2 adsorption–desorption isotherms obtained at 77 K, using an ASAP 2010 surface area analyzer.

3. Results and discussion

3.1. Morphology and structure of the NCS

Fig. 1a shows a typical low-magnification SEM image for NCS-H. A quantity of clean carbon spheres, with a perfect spherical morphology, can be clearly observed. The close-up SEM and TEM images in Fig. 1b and c, respectively, indicate a clear solid structure for NCS-H, with a smooth surface and a narrow diameter ranging from 130 to 180 nm. The HRTEM image at the edge of the NCS-H, in Fig. 1d, indicates short and disordered graphite layers for NCS-H, which are separated by ~0.34 nm. Fig. 1e displays the XRD pattern for NCS-H, where the two peaks at 25.0° and 43.8°, can be assigned as typical graphitic (0 0 2) and (1 0 0) planes, respectively. The broadening of the two peaks suggests a low graphitization degree. This result is coincident with the observations from HRTEM. The BET surface areas of NCS-H were found to be 12.8 m^2 g^{-1}. The XPS wide spectra for NCS-H, in Fig. 1f, show the presence of principal C$_{1s}$, O$_{1s}$, and N$_{1s}$ core levels, with no evidence of any other elements. The elemental content analysis from the XPS data reveals a composition (wt.%) of: C 89.5, N 6.2, O 4.3, for NCS-H.

3.2. Electrocatalytic activity, stability and methanol tolerance of the NCS

To investigate the electrocatalytic activity of NCS-H, the cyclic voltammograms of NCS-H in 0.1 M KOH solutions saturated with N_2 or O_2 were performed. When the electrolyte solution was saturated with O_2, as shown in Fig. 2a, a distinct peak at −0.29 V, corresponding to an O_2 reduction reaction, can be observed. This result suggests that NCS-H exhibits an excellent catalytic activity towards the ORR. The stabilities and possible crossover effects of the catalyst materials are also very important from a practical application perspective. Therefore, the electrocatalytic selectivity of NCS-H was measured versus the electro-oxidation of methanol. From Fig. 2a, no noticeable change in ORR current density is observed at the NCS-H electrode, after the addition of 3 M methanol in 0.1 M KOH. This indicates that the NCS-H bears a high selectivity towards the ORR, with no significant crossover effects. The durabilities of the NCS-H and Pt/C catalysts were compared. The catalysts were held at −0.35 V for 8000s in an O_2 saturated 0.1 M KOH solution, with an agitation rate of 1600 rpm. From Fig. 2b, the NCS-H has a superior durability compared with the Pt/C catalyst. These results confirm that NCS-H holds high promise for use in methanol and alkaline fuel cells.

3.3. Studying the ORR electrochemical procedures of the NCS

To further probe the role of NCS-H throughout the ORR electrochemical process, we performed a RDE experiment. The RDE current-potential curves, at various rotating speeds (from 400 to
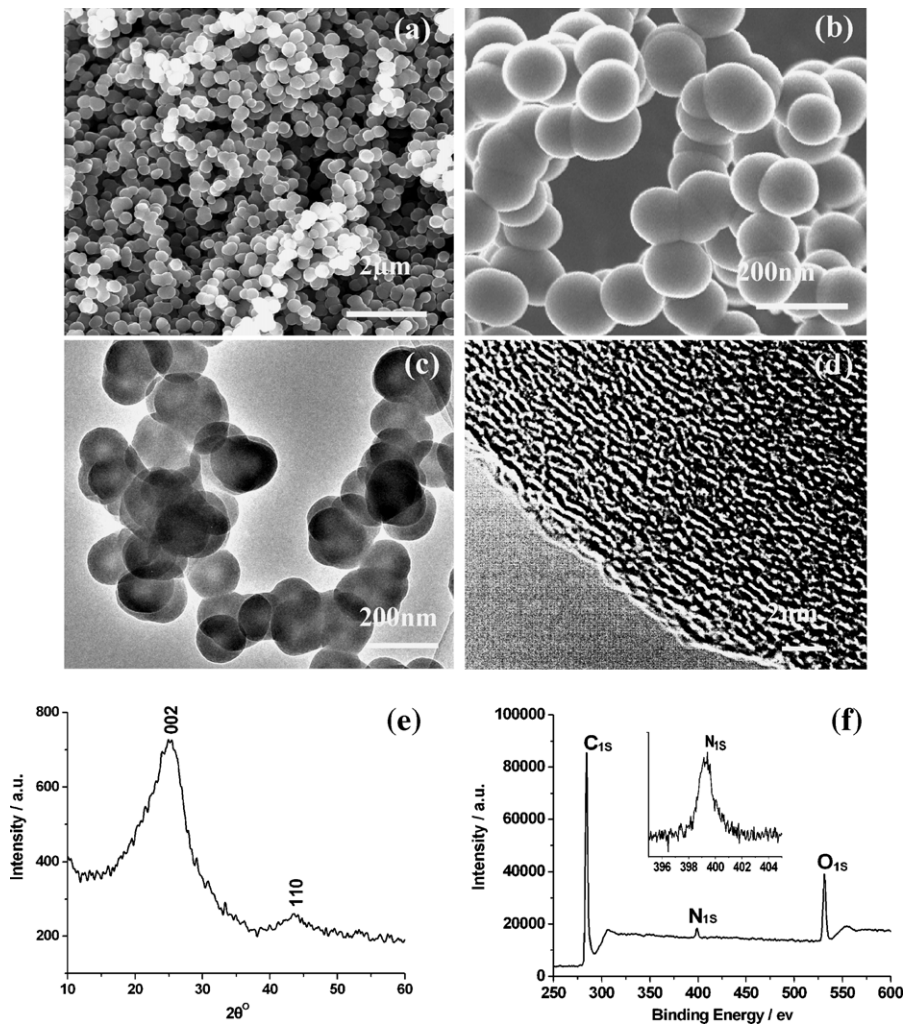
Fig. 1. SEM (a and b), TEM (c) and HRTEM (d) images, and XPS (e) and XRD (f) curves for NCS-H.

3600 rpm), are shown in Fig. 3a. The limited diffusion current densities are dependent on the rotating rates. The corresponding Koutecky–Levich (K–L) plots (J^{-1} versus $\omega^{1/2}$), at various electrode potentials, exhibit a good linearity as shown in Fig. 3b. The number of electron transfers involved in the ORR can be calculated from the K–L equation:

$$J^{-1} = J_L^{-1} + J_K^{-1} = (B\omega^{1/2})^{-1} + J_K^{-1} \tag{1}$$

$$B = 0.62nFC_0(D_0)^{2/3}\nu^{-1/6} \tag{2}$$

$$B = nFkC_0 \tag{3}$$

where J is the measured current density, J_K and J_L are the kinetic- and diffusion-limiting current densities, ω is the angular velocity of the disk ($\omega = 2pN$, N is the linear rotation speed), n is the overall number of electrons transferred in the oxygen reduction, F is the Faraday constant ($F = 96,485$ C mol^{-1}), C_0 is the bulk concentration
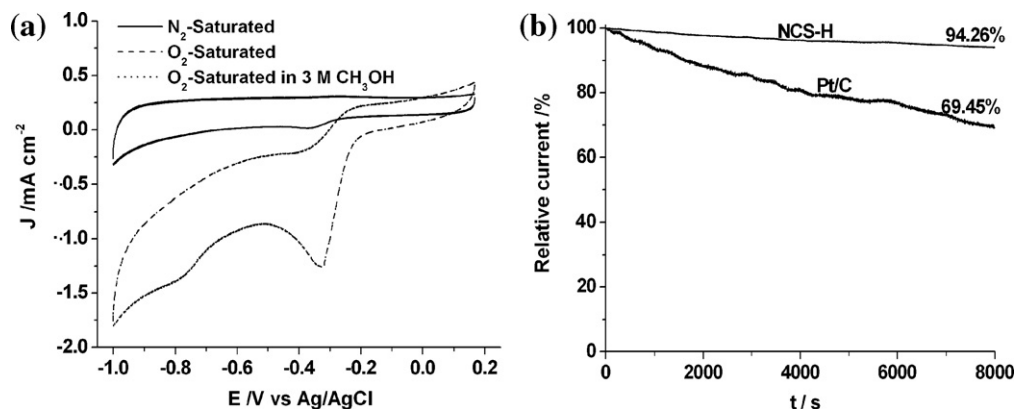

Fig. 2. Cyclic voltammograms for (a) NCS-H and (b) the Pt/C catalyst for oxygen reduction in a 0.1 M KOH solution, saturated with N$_2$ or O$_2$, at a scan rate of 50 mV s^{-1}. (c) Current–time (i–t) and chronoamperometric responses of the NCS-H and Pt/C-modified GC electrodes, at −0.35 V in an O$_2$-saturated 0.1 M KOH, at a rotation rate of 1600 rpm.
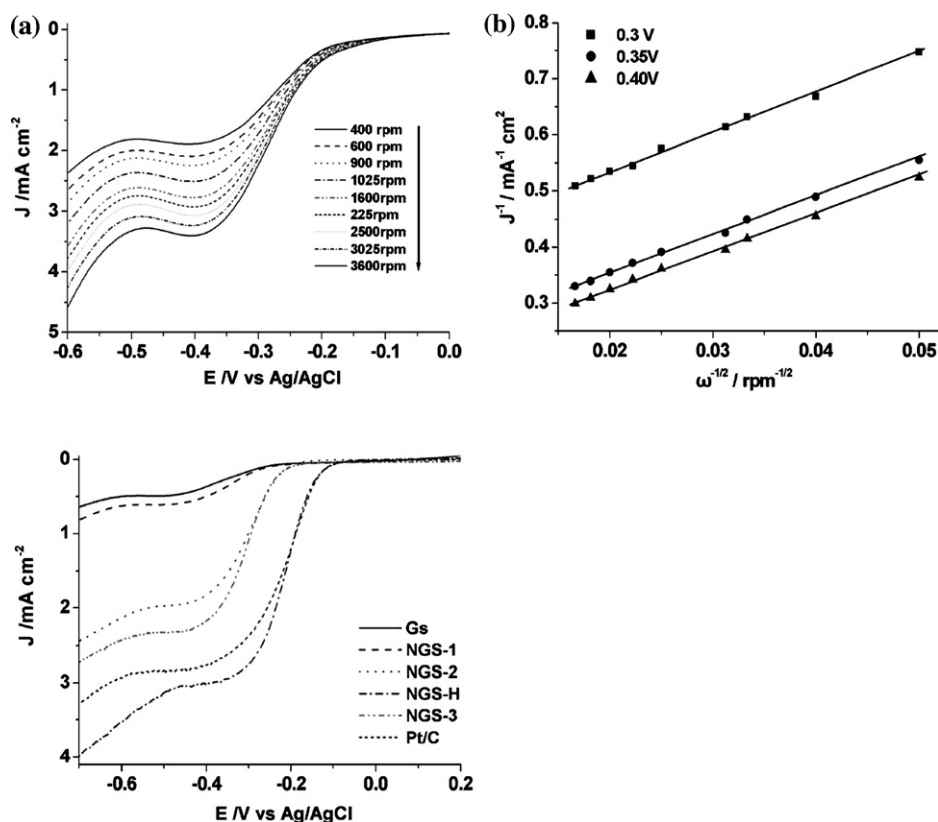
Fig. 3. (a) Rotating-disk voltammograms for the NCS-H electrode in an O_2-saturated 0.1 M solution of KOH, at a scan rate of $10\,mV\,s^{-1}$, for different rotation rates. (b) Koutecky–Levich plot (J^{-1} versus $\omega^{1/2}$) at different electrode potentials. Experimental data were obtained from (a). (c) Polarization curves for various carbon spheres and a Pt/C catalyst on a glass carbon rotating disk electrode saturated in O_2, at a scan rate of $10\,mV\,s^{-1}$ and a rotation rate of 1600 rpm.

of O_2 ($C_0 = 1.2 \times 10^{-6}\,mol\,cm^{-1}$), ν is the kinematic viscosity of the electrolyte ($\nu = 0.01\,cm^2\,s^{-1}$), and D_0 is the diffusion coefficient of O_2 in 0.1 M KOH ($1.9 \times 10^{-5}\,cm^2\,s^{-1}$). According to Eqs. (1) and (2), the number of electron transfers (n) is calculated to be 3.86 at $-0.35\,V$, indicating that a four-electron-transfer reaction is required to directly reduce oxygen to OH^-. The calculated J_K value of $5.21\,mA\,cm^{-2}$ at $-0.35\,V$ is slightly higher than that for the Pt/C catalyst ($4.36\,mA\,cm^{-2}$). These results further confirm that NCS-H is a promising NPMC with a high catalytic activity for the ORR.
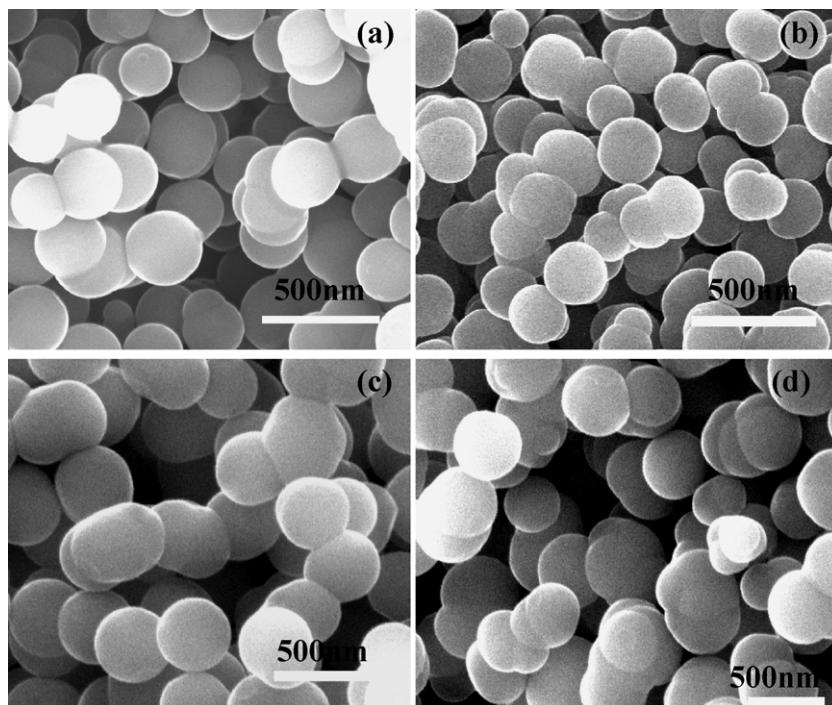

Fig. 4. SEM images of (a) CS, (b) NCS-1, (c) NCS-2 and (d) NCS-3.

3.4. Effect of the NCS physical parameters on the electrocatalytic activity

To investigate the influence of the NCS physical parameters (N content, specific surface area value) on the electrochemical properties, various NCS were studied using linear voltamperometry, at a rotation rate of 1600 rpm, and compared with the Pt/C catalyst. Fig. 3c shows the polarization curves for these different materials in an O_2 saturated 0.1 M KOH solution. Their SEM images are shown in Fig. 4. The physical parameters, electrochemical properties and corresponding experimental data are listed in Table 1. From Fig. 3c, all NCS have a more positive onset potential and a higher limiting current density than non-nitrogen CS. This result strongly confirms that nitrogen doping is very important for a high catalytic activity. The C–N structure within NCS may also play a decisive role in the ORR activity enhancement. Upon comparing the polarization curves of the NCS (NCS-H, NCS-1, NCS-2 and NCS-3), we observed that NCS-H exhibits the highest electrocatalytic activity. From their physical parameters, as listed in Table 1, it can be concluded that a high nitrogen content and high specific surface area value are key for high activity. Similar observations have been previously reported [16]. Furthermore, from Fig. 3c, the onset potential for NCS-H is close to that of the Pt/C catalyst, but the current density at −0.6 V is higher. These results further confirm that NCS-H has a high catalytic activity towards the ORR.

4. Conclusion

In summary, large-scale NCS have been successfully synthesized via a catalyst-free spray pyrolysis method. The NCS exhibit excellent electrocatalytic activities, long-term stability, and a high methanol tolerance in alkaline medium, compared with Pt/C catalysts. We have successfully developed a new NPMC, with an excellent electrocatalytic performance, using a simple, cost-effective and scalable method. We have also provided an increased understanding in the origins of the ORR activity enhancements using NCMs.

Acknowledgements

References

[1] B. Lim, M.J.P. Jiang, E.C. Cho, J. Tao, X.M. Lu, Y.M. Zhu, Y.N. Xia, Science 324 (2009) 1302.
[2] A. Serov, C. Kwak, Appl. Catal. B: Environ. 90 (2009) 313.
[3] R. Jasinski, Nature 201 (1964) 1212.
[4] K.P. Gong, F. Du, Z.H. Xia, M. Durstock, L.M. Dai, Science 323 (2009) 760.
[5] S.S. Yu, Q. Zhang, L.M. Dai, J. Am. Chem. Soc. 132 (2010) 15839.
[6] W. Xiong, F. Du, Y. Liu, A. Perez, M. Supp, T.S. Ramakrishnan, L.M. Dai, L. Jiang, J. Am. Chem. Soc. 132 (2010) 15839.
[7] T.C. Nagaiah, S. Kundu, M. Bron, M. Muhler, W. Schuhmann, Electrochem. Commun. 12 (2010) 338.
[8] Y.F. Tang, B.L. Allen, D.R. Kauffman, A. Star, J. Am. Chem. Soc. 131 (2009) 13200.
[9] R.L. Liu, D.Q. Wu, X.L. Feng, K. Mullen, Angew. Chem. Int. Ed. 49 (2010) 2565.
[10] L.T. Qu, Y. Liu, J.B. Baek, L.M. Dai, ACS Nano 4 (2010) 1321.
[11] W. Yang, T.P. Fellinger, M.J. Antonietti, J. Am. Chem. Soc. 133 (2011) 206.
[12] D.S. Yu, L.M. Dai, J. Phys. Chem. Lett. 1 (2010) 467.
[13] T. Ebbesen, P. Ajayan, K. Tanigaki, Nature 367 (1994) 519.
[14] L.M. Cele, N.J. Coville, Carbon 47 (2009) 1824.
[15] Z. Yang, X.H. Chen, H.G. Nie, K. Zhang, L.S. Xu, B. Yi, Nanotechnology 19 (2008) 5606.
[16] Z. Chen, D. Higgins, H. Tao, R.S. Hsu, Z.W. Chen, J. Phys. Chem. C 113 (2009) 21008.